

# Effect of composition on transport properties of $\text{Ge}_{10}\text{As}_x\text{Te}_{90-x}$ chalcogenide system

A M Ahmed, M M Wakkad, S H Mohamed\* and A K Diab

Department of Physics, Faculty of Science, Sohag University, Sohag 82524, Egypt

Received: 26 August 2012 / Accepted: 21 November 2012 / Published online: 6 December 2012

**Abstract:** Chalcogenide bulk alloys of  $\text{Ge}_{10}\text{As}_x\text{Te}_{90-x}$  ( $x = 20, 25, 30, 35, 40, 45$  and  $55$ ) system were prepared by the conventional melt quench-technique. The dc electrical conductivity  $\sigma$  and thermoelectric power (TEP) measurements were carried out in the temperature ranges from 83 to 353 K and from 253 to 353 K, respectively. The variations of both  $\sigma$  and TEP with temperature proved n-type semiconducting behavior of these materials. The current density–electric field characteristics were found to be linear. In addition, the value of negative Seebeck coefficient was decreased with increasing As content. The activation energies, calculated for both electrical conductivity  $E_\sigma$  and thermoelectric power  $E_S$ , were composition dependent.

**Keywords:** Alloys; Chalcogenides; Electrical conductivity; Seebeck coefficient

**PACS Nos.:** 61.43.Dq; 66.10.Ed; 72.15.Cz; 72.15.Jf

## 1. Introduction

Many approaches have been proposed to explain the compositional dependence of various physical properties of chalcogenide network glasses [1–9]. One of these approaches is the so-called chemically ordered network model (CONM) [1], in which the formation of heteropolar bonds is favored over the formation of homopolar bonds. In this model, the glass structure is assumed to be composed of cross-linked structural units of the stable chemical compounds (heteropolar bonds) of the system and excess, if any, of the elements (homopolar bonds). Due to chemical ordering features such as extremum, a change in slope or kink occurs for the various properties at the so-called tie line or stoichiometric compositions [10]. At these compositions the glass structure is made up of cross-linked structural units consisting of heteropolar bonds only.

The electrical properties of glassy  $\text{As}_x\text{Ge}_{10}\text{Te}_{90-x}$  alloys have been studied [11]. The dc conductivity of investigated alloys was expressed as a sum of two activated processes in which one dominated at higher temperatures and the other dominated at low temperatures. The high temperature activation energy depends on arsenic content while the lower

temperature activation energy seems to be due to some basic mechanisms independent of composition. The observation of temperature independence of the ac conductivity at lower temperatures and the effect of the applied field on the dc conductivity support the evidence of defect states in the gap. The “variable-range hopping” was not present in these glasses. The qualitative explanation was also given on the basis of the dangling-bond theory for the observed conductivity and dielectric behaviour of As–Ge–Te glasses. Also, the electrical conductivity and the phenomenology of switching in the  $\text{Ge}_{0.09}\text{As}_{0.20}\text{Te}_{0.71}$  glassy alloy were studied [12]. It was suggested that the electrical parameters are subject to the same statistical variations that are found in any other fabrication and characterization process in Ge–AsTe alloys. The role of electrical power on the phenomenon under study suggests that the effects of thermal process origin dominate in the observed switching effect. For the discussion of the conductivity mechanisms of amorphous semiconductors, it is relevant to know whether electrons or holes predominate in the transport [13]. To obtain this knowledge measurements of thermoelectric power are frequently used, because its sign is closely related to the charge of the dominating carriers. The temperature dependence of thermoelectric power measurements together with those of the dc conductivity gives further information about the transport mechanisms.

\*Corresponding author, E-mail: abo\_95@yahoo.com

There are numerous applications of the Ge–As–Te chalcogenide alloy system due to its excellent structural, optical and electrical properties. It has been shown that memory switching devices can be made from the Ge–As–Te glasses. The memory switching devices have many potential applications such as the control of the electroluminescent display panels and the read only memories [14]. Prakash et al. [15] have investigated the easily reversible memory switching in Ge–As–Te glasses. The memory state of these samples is found to be easily reversible, which indicates the suitability for read memory applications. Mehra et al. [16] found that the activation energy of crystallization decreased with increasing As content. It is therefore suggested that the materials with lower concentration of Ge (<10 %) and As and Te concentrations between (35–55 at.%) are of considerable importance for reversible phase change optical recording applications. Recently, Yang et al. [17] found that Ge–As–Te and Ge–As–Te–Cu glasses are promising candidates for bio-optical detection applications.

This paper reports the electrical conductivity and thermo-electric power of the glassy  $\text{As}_x\text{Ge}_{10}\text{Te}_{90-x}$  compositions. The conduction behaviour and the electrical parameters are identified from the electrical conductivity measurements. The nature of charge carriers as well as the activation energy of TEP is determined from the thermoelectric power measurements. One result is that the alloys in the bulk form are useful thermoelectric energy converts.

## 2. Experimental details

The  $\text{Ge}_{10}\text{As}_x\text{Te}_{90-x}$  ( $x = 20, 25, 30, 35, 40, 45$  and  $55$ ) glasses were prepared by the standard melt quenching method as described in [18, 19]. Typical, 10 g total (per batch) of appropriate quantities of 99.999 % pure germanium (Ge), arsenic (As) and tellurium (Te) were weighed and charged into cleaned silica ampoules with inner diameter of 1 cm. The ampoules were evacuated to  $10^{-5}$  torr and sealed under this vacuum. The ampoules were held at a temperature of 1,100 °C for about 12 h, at the end of which the ampoules were quenched in iced water to obtain glasses. During the preparation the ampoules were continuously rotated to ensure complete mixing of the various constituents. The disk shaped samples with a diameter equal to 1 cm and thickness equal to 0.2 cm were obtained. The crystallinity of the as-prepared glasses was examined using a Philips X'pert MRD diffractometer.  $\text{CuK}_\alpha$  radiation ( $\lambda = 1.541837 \text{ \AA}$ ) was used from the X-ray tube with normal theta-2theta scan.

The measurements of the dc electrical conductivity and current–voltage characteristics were carried out using a pressure contact sample holder. The adjacent parallel surfaces of the samples were painted with silver paste as contact electrodes. A conventional series current circuit was

used. The current was measured by using an electrometer (Keithley model 610C), while the potential difference was measured by means of Keithley 175 microvoltmeter. A copper-constantan thermocouple was used for monitoring the temperature. The thermoelectric power measurements were carried out using a differential temperature sample holder ended with two graphite electrodes. The difference in temperature between the two opposite surfaces of the samples was equal to 3 °C during the whole measurements. The thermoelectric power (TEP) voltage was measured by using Hewlett Packard 3441 A multimeter.

## 3. Results and discussion

The X-ray diffraction was used to study the effect of arsenic content on the amorphous nature of the materials. Figure 1 shows the X-ray diffractograms of the as-prepared  $\text{Ge}_{10}\text{As}_x\text{Te}_{90-x}$  compositions. The general feature of these diffractograms is characterized by the presence of three humps emphasizing the amorphous structure of all compositions. The first diffraction hump (FDH) located at  $2\theta \sim 12^\circ$ , is attributed to the medium-range structural order [20]. The second ( $2\theta \sim 29^\circ$ ) and the third ( $2\theta \sim 50^\circ$ ) humps results from the correlation between the second nearest neighbors and the third nearest neighbors [21]. Lippens et al. [22] and Vazquez et al. [23] have prepared  $\text{Ge}_{10}\text{As}_{20}\text{Te}_{70}$ ,  $\text{Ge}_{10}\text{As}_{46}\text{Te}_{54}$ ,  $\text{Ge}_{10}\text{As}_{54}\text{Te}_{36}$  and  $\text{Ge}_5\text{As}_{20}\text{Te}_{75}$ ,  $\text{Ge}_{10}\text{As}_{20}\text{Te}_{70}$ ,  $\text{Ge}_{14}\text{As}_{43}\text{Te}_{43}$  glasses, respectively, using the direct melt quenching technique in an ice-water bath. However, Ramesh [24] affirmed the difficulty of obtaining glasses from  $\text{Ge}_{10}\text{As}_x\text{Te}_{90-x}$  using the direct melt quenching technique. This inconsistency may be related to the difference in preparation conditions, where in Ramesh's work the temperature of the melt was reduced to 850 °C before quenching the melt in ice water and NaOH mixture.

It is worth to mention that Narayanan et al. [18] have experimentally found that the Ge–As–Te glass was formed easily for the compounds with mean-coordination number of atoms  $\langle r \rangle = 2.40$  and 2.67. Lippens et al. [22] have studied electronic structure of  $\text{Ge}_{0.1}\text{As}_x\text{Te}_{0.9-x}$  glasses by extended X-ray absorption (XAS) fine structure spectroscopy which confirmed the increase of the short-range disorder with increasing As content. They observed a decrease in the amplitude of the XAS peak with increasing As content. This decrease of the amplitude of the XAS peak was clearly related to the increase of the As content and could be due to differences between the electronic transition probabilities from the As 1s core state to the p-type anti-bonding states for As–As and As–Te molecules. Since the first of our compositions has  $\langle r \rangle$  value of 2.40 and the As content increases as x increases, these results may favor the formation of the amorphous structure of our compositions.

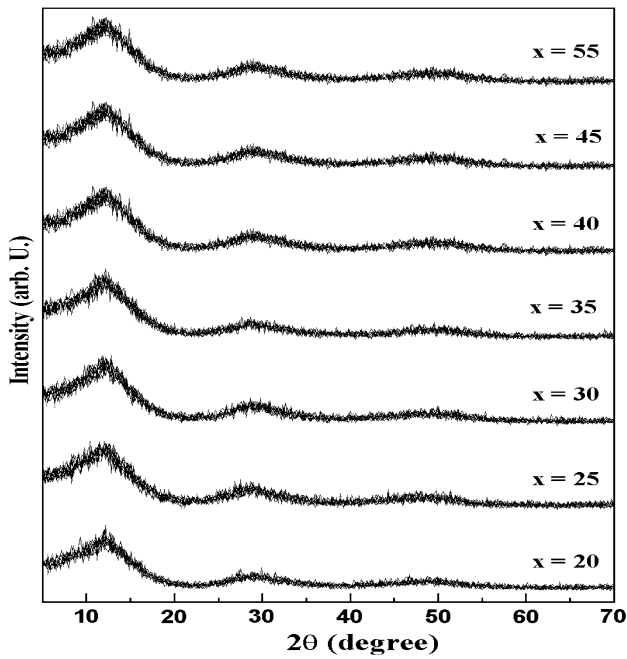


Fig. 1 X-ray diffraction patterns for  $\text{Ge}_{10}\text{As}_x\text{Te}_{90-x}$  bulk materials

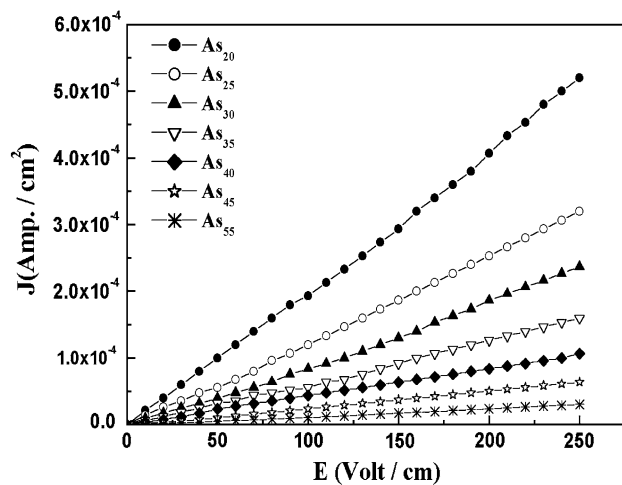


Fig. 2 The relation between the current density ( $J$ ) and the electric field ( $E$ ), measured at room temperatures for compositions

The current density ( $J$ )-electric field ( $E$ ) characteristics of the as-prepared bulk specimens of the  $\text{Ge}_{10}\text{As}_x\text{Te}_{90-x}$  chalcogenide system with  $20 \leq x \leq 55$  were investigated at 83, 153, 203, 300, 333 and 353 K. Figure 2 shows the  $J$  versus  $E$  plots measured at room temperature (300 K) for as-prepared compositions. It is seen that the general feature of the  $J$ - $E$  characteristics is linear in the most of the range of the applied electric field. Moreover, the current density increases consistently with decreasing As concentration. This indicates that, the resistivity of composition increases as the increasing As content. This increase of  $\rho$  can be

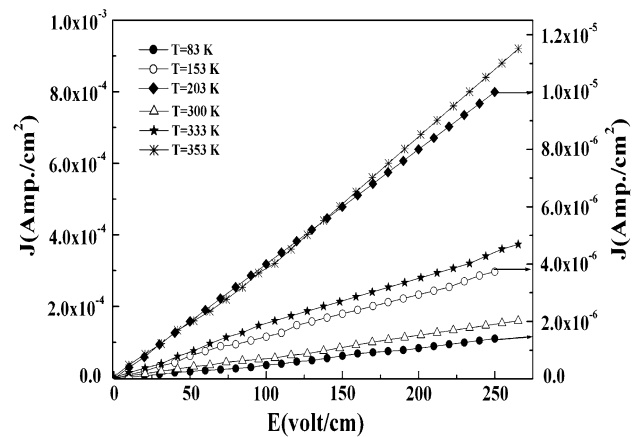


Fig. 3 The relation between the current density ( $J$ ) and the electric field ( $E$ ) measured at different ambient temperatures for  $\text{Ge}_{10}\text{As}_{35}\text{Te}_{55}$  composition

attributed to the transformation of the excess chain-like Te into three dimensional structural species as a result of the interaction of As with Ge and Te [18].

Figure 3 shows the  $J$ - $E$  characteristics of the as-prepared sample with  $x = 35$  at.%. The measurements were carried out at different temperatures. This figure reveals that the  $J$ - $E$  characteristics are nearly linear. This confirms the temperature enhancement of the electrical conductivity. On the other hand, the effect of the applied electric field is more pronounced especially in its relatively higher range. The above findings indicate that the electrical conductivity can be enhanced by both the temperature and the electric field, and the role of  $T$  is more pronounced at higher values of  $E$ .

Regarding the different  $J$ - $E$  characteristics, the following conclusions can be drawn.

- The general feature is that of ohmic conduction (linear characteristics) for the most range of  $E$ .
- The electrical conductivity shows field dependence especially at the relatively higher field range.

For the seven compositions, the double logarithmic relation between  $J$  and  $E$ , measured at different temperatures, is linear exhibiting one slope. However, the plots on this figure are suitable of the power relation to describe the dependence of  $J$  and  $E$ , which can be formulated empirically as following [6]:

$$J = CE^n \quad (1)$$

The values of  $n$  were calculated for all the compositions and at different temperatures. It is found that the value of the exponent  $n$  is in between 0.97 and 1.02, so that it can be approximated to unity for all samples and temperatures.

The variation of dc conductivity with the reciprocal of temperature in the range of 83–353 K for the  $\text{Ge}_{10}\text{As}_x\text{Te}_{90-x}$  compositions, where  $20 \leq x \leq 55$ . It is seen that  $\sigma$

increases with increasing  $T$  for all compositions. Hence, the investigated compositions behave as a semiconducting material. At any given temperature the dc conductivity decreases with increasing As content, which can be attributed to the microstructural changes with increasing the latter. It was previously [22] reported that the main structural changes with increasing As content are due to: (i) the increase in the number of As–As bonds and the decrease in the number of As–Te bonds and (ii) the increase of the short-range disorder (bond length distribution). The former structural change could explain the observed collapse if the bonding energy of the As–As bonds is greater than that of the As–Te bonds by about 1 eV which is possible.

The electronic transitions from the As  $1s$  state to the As  $p$ -type empty states are compared to the anti-bonding states of the As–Te and As–As bonds involving the As  $4p$  states [22]. Differences between the electronic transition probabilities from the As  $1s$  core state to the  $p$ -type anti-bonding states for As–As and As–Te molecules [25] and the cross-linking effect of As on Te chains as well as by the increase of density of stronger bonds with As content in the structure of system studied [26]. Also it can be attributed to the transformation of the excess chain-like tellurium into three dimensional structural species as a result of the interaction of As with Ge and Te. The weak Van der Waals bonds between the chains are replaced in this case by rigid covalent bonds and the glass structure becomes stronger [19], and the low values of conductivity for such a system suggests the extensive participation of localized states near the mobility edges in the conduction process at room temperature [27].

It can be concluded from Fig. 4 that the conduction phenomena of the investigated glasses proceeds through the following two distinct conduction channels:

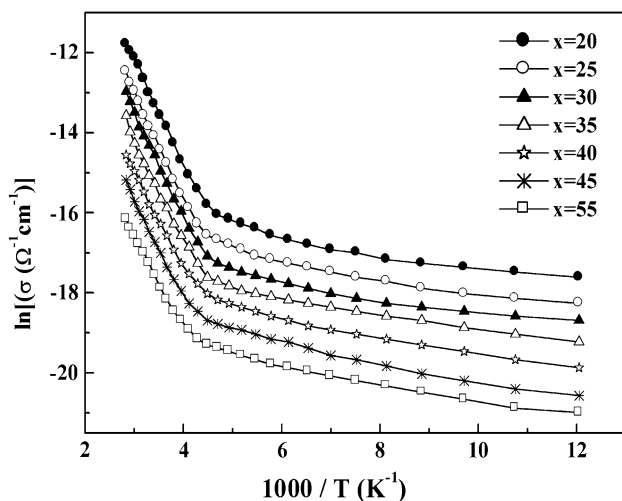


**Fig. 4** The temperature dependence of the electrical conductivity for  $\text{Ge}_{10}\text{As}_x\text{Te}_{90-x}$  compositions

- (i) At relatively higher range of temperature ( $T > 233$  K) the conductivity is strongly dependent on  $T$ . This represents the conduction through the extended states. In this case, the dependence of  $\sigma$  on  $T$  can be represented by the well-known Arrhenius formula [28]:

$$\sigma = \sigma_o \exp(-E_e/k_B T) \quad (2)$$

where  $\sigma_o$  is the pre-exponential factor (which includes the carrier mobility and density of states),  $E_e$  is the corresponding activation energy of electrical conductivity (which is a function of the electronic energy levels of the chemical interacting atoms in the glass) and  $k_B$  is the Boltzmann constant. Figure 5 shows the fitted linear data of high temperature range of Fig. 4, which gives the values of both  $E_e$  and  $\sigma_o$ , for the investigated compositions, summarized in Table 1.  $E_e$  increases continuously with increasing As ratios. However, these results are in good agreement with those obtained by other authors [27, 29]. The observed results may be attributed to the probability of release of the carriers from the localized states due to the thermal excitation. As the As content decreases, the ratio of Te and the number of ionic pairs might increase. This may cause a broadening in the localized energy levels. In turn, this might cause a narrowing in the energy gap. Consequently, one might expect a decrease in the activation energy of conduction as the As content decreases.

- (ii) The conductivity data in the low temperature region  $T \leq 223$  K show that the conductivity is slightly dependent on temperature, which is the behaviour of conduction through localized states. In this case the dependence of the conductivity on the temperature can be described according to Mott's formula [30] for

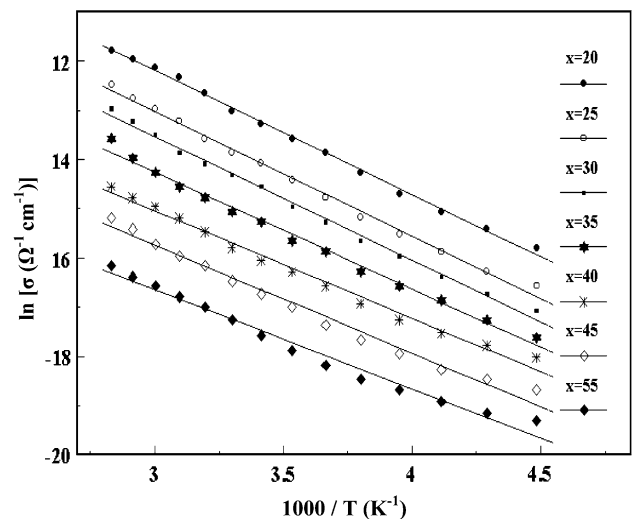


**Fig. 5** Plots of  $\ln(\sigma)$  versus  $1,000/T$  for  $\text{Ge}_{10}\text{As}_x\text{Te}_{90-x}$  compositions

**Table 1** Variations of  $E_c$  (eV) and  $\sigma_o$  ( $\Omega^{-1} \text{ cm}^{-1}$ ) with As content for the  $\text{Ge}_{10}\text{As}_x\text{Te}_{90-x}$  compositions

x (at.%)	20	25	30	35	40	45	55
$E_c$ (eV)	0.297	0.316	0.334	0.356	0.367	0.371	0.382
$\sigma_o$ ( $\Omega^{-1} \text{ cm}^{-1}$ )	81.363	54.267	41.843	36.853	25.737	15.347	9.457

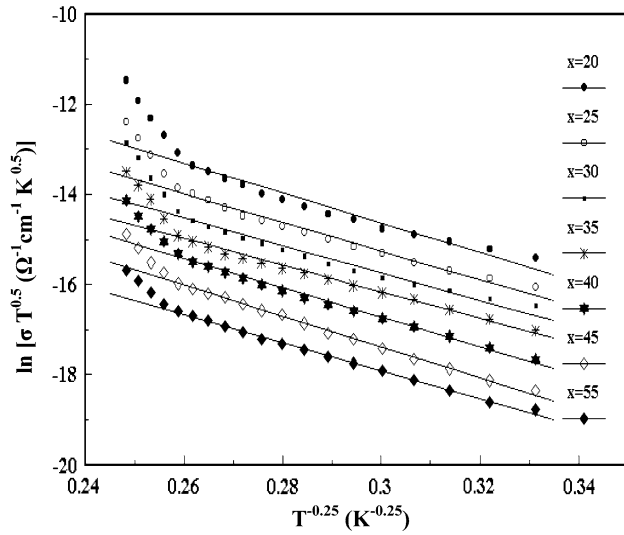
variable-range hopping (VRH) conduction. In Mott's theory the temperature dependent conductivity is given by the formula:

$$\sigma\sqrt{T} = \sigma'_o \exp\left(-B/T^{1/4}\right) \quad (3)$$

with

$$B = T_o^{1/4} = 1.66 \left[\alpha^3/k_B N(E_F)\right]^{1/4} \quad (4)$$

where  $\sigma'_o$  is a pre-exponential factor,  $\alpha$  is the coefficient of exponential decay of the localized state wavefunction, which is assumed to be  $0.124 \text{ \AA}^{-1}$  and  $N(E_F)$  is the density of localized states (DOLS) at the Fermi level.

**Fig. 6** Plots of  $(\ln \sigma T^{0.5})$  versus  $T^{-0.25}$  for  $\text{Ge}_{10}\text{As}_x\text{Te}_{90-x}$  compositions**Table 2** Variations of  $N(E_F)$  ( $\text{cm}^{-3} \text{ eV}^{-1}$ ),  $N$  ( $\text{cm}^{-3}$ ),  $R_{av}$  ( $\text{\AA}$ ),  $W$  (eV) and  $\sigma'_o$  ( $\Omega^{-1} \text{ cm}^{-1} \text{ K}^{1/2}$ ) as functions of compositions for  $\text{Ge}_{10}\text{As}_x\text{Te}_{90-x}$  chalcogenide system

x (at.%)	$N(E_F) \times 10^{-20}$ ( $\text{cm}^{-3} \text{ eV}^{-1}$ )	$N \times 10^{-18}$ ( $\text{cm}^{-3}$ )	$R_{av}$ ( $\text{\AA}$ )	$W$ (meV)	$\sigma'_o \times 10^5$ ( $\Omega^{-1} \text{ cm}^{-1} \text{ K}^{1/2}$ )
20	0.980	5.064	3.448	59.419	4.534
25	1.036	5.359	3.400	58.585	2.136
30	1.301	6.728	3.212	55.346	0.790
35	1.423	7.358	3.141	54.120	0.732
40	0.893	4.619	3.529	60.800	0.693
45	0.689	3.564	3.765	64.872	0.676
55	1.006	5.201	3.426	59.023	0.162

Figure 6 shows the fits of the data in temperature range  $T \leq 223 \text{ K}$  to Mott's relation (Eq. (3)) for  $\text{Ge}_{10}\text{As}_x\text{Te}_{90-x}$  compositions. The parameters of variable range hopping conduction, namely, the density of localized states (DOLS) at the Fermi level  $N(E_F)$ , are calculated from the slopes of the lines of Fig. 6. The parameters are, then, used to calculate the hopping distance ( $R_{av}$ ) and the hopping energy ( $W$ ). In Mott's theory  $R_{av}$  and  $W$  are given by:

$$R_{av} = \left[\frac{9}{8\pi\alpha N(E_F)k_B T}\right]^{1/4} \quad (5)$$

$$W = \frac{3}{4\pi R_{av}^3 N(E_F)} = \left[\frac{2\alpha^3 k_B^3 T^3}{9\pi N(E_F)}\right]^{1/4} \quad (6)$$

The concentration of conduction electrons ( $N$ ) within a range of  $k_B T$  of the Fermi energy can be calculated from  $2k_B T N(E_F)$  [31]. The values of  $N(E_F)$ ,  $N$ ,  $R_{av}$  and  $W$  for  $\text{Ge}_{10}\text{As}_x\text{Te}_{90-x}$  compositions are calculated and recorded in Table 2. The obtained  $N(E_F)$  and  $N$  data do not sequentially change with the investigated compositions. As shown in this Table, the values of  $N(E_F)$  and  $N$  have a maximum at  $x = 35$  at.% and both  $R_{av}$  and  $W$  have a maximum at  $x = 45$  at.% and vice versa. In the other side, the values of  $\sigma'_o$  were decreased with increasing As content. Besides, these values are high compared with those recorded previously [32–34] for some chalcogenide glasses. The small values of both  $R$  and  $W$  recorded in Table 2, which are approximately satisfy the conditions of Mott's VRH process;  $\alpha R_{av} \gg 1$  and  $W > k_B T$ , can be attributed to the obtained unreasonably high values of  $N(E_F)$ . The disparities in  $N(E_F)$  evaluation have been also observed for some semiconducting materials [35] and have been attributed to the incorrect assumptions of Mott's derivation of VRH relations such as the energy independence of the

density of localized state at the Fermi level, neglect of the correlation effect in tunneling process and neglect of electron–phonon interaction.

Figure 7 shows the plots of Seebeck coefficient  $S$  versus the reciprocal temperature for the seven compositions. It is seen in this figure that within the entire temperature range for measurements ( $133 \leq T \leq 353$  K), the generated thermoelectric power (TEP) possessed negative sign similar to typical n-type semiconductors. Such negatives Seebeck values confirm that the contribution to the observed TEP is mainly due to electrons. These results are not in agreement with Borizova [36] and Kolobov [37], who reported that the p-type conductivity in amorphous chalcogenides is given based on the role played by lone-pair electrons and charged defects. Valency alternation results in thermal excitation of free holes while free electrons are not created. Neutral dangling bonds are also a source of free holes. However in our case, the contributions electrons are thermally activated. The continuous decrease of the negative magnitudes of the Seebeck coefficient with inhabitation of temperature emphasizes that, the investigated materials are with mixed carriers. Besides, the concentration of negative carriers (electrons) decreased with increasing As content. This is may be due to the differences between the electronic transition probabilities from the As  $1s$  core state to the p-type anti-bonding states; or perhaps,

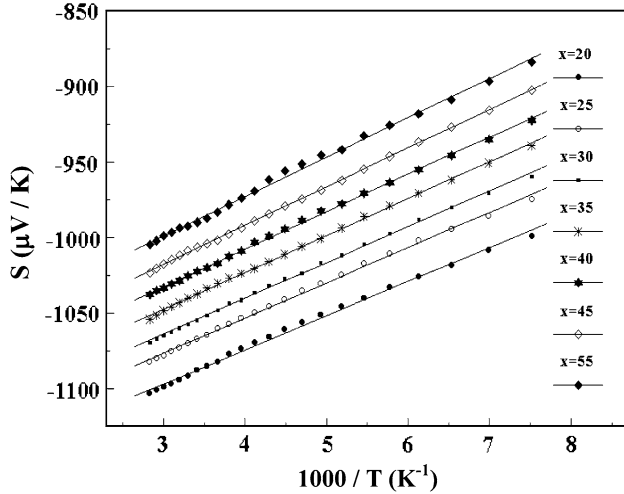


**Fig. 7** The temperature dependence of Seebeck coefficient for  $\text{Ge}_{10}\text{As}_x\text{Te}_{90-x}$  compositions

the material transformation to p-type semiconductors was increased with the increase of the As content. Hence, it may be concluded that both the thermally activated electrons and holes contribute to the observed thermoelectric power. It is worth mentioning that the p–n transition has been reported previously in some chalcogenide glasses [38–41]. The linear plots shown in Fig. 7 indicate that the temperature dependence of Seebeck coefficient can be described by the following equation [42, 43]:

$$S = \pm \frac{k_B}{e} \left( \frac{E_s}{k_B T} + A \right) \quad (7)$$

where  $A$  is a dimensionless parameter which relates to the carrier scattering mechanism [30] or assumed to be a measure of the kinetic energy transported by carrier [44]. The plus and minus sign hold for the p-type and n-type semiconductors, respectively. As mentioned earlier,  $S$  possessed negative sign for all the investigated compositions within the whole considered range of temperature.

Slopes of the  $S$  versus  $1/T$  plots possessed positive sign confirming the decrease of electron contribution to the activation with increasing  $T$  which confirms in turn that, transition of material to p-type with dominant activation of holes is unexpected at higher temperatures. Therefore, application of the above equation permits us to calculate both the electrochemical potential  $E_s$  and dimensionless parameter  $A$  which are recorded in Table 3. It is seen that the values of  $E_s$  decreases with increasing As content. This may be attributed to the decrease of electrons, which in turn resulted from the increase in As content. On the other hand, the parameter  $A$  possessed anomalously high values which are unusual for normal semiconductors. However this observation may be attributed to the relatively higher effective mass of holes compared to those of electrons.

#### 4. Conclusions

The XRD characteristics of as prepared  $\text{Ge}_{10}\text{As}_x\text{Te}_{90-x}$  chalcogenide compositions prove the amorphous nature for all compositions. From the electrical conduction, it can be extracted that:

- The  $J$ – $E$  characteristics are linear for the most rang of  $E$ .
- The electrical conductivity decreases with increasing content of As, which has been attributed to the microstructural changes with increasing As content.

**Table 3** Variations of the activation energy of Seebeck coefficient  $E_s$  ( $\mu$  eV) and the parameter  $A$  for  $\text{Ge}_{10}\text{As}_x\text{Te}_{90-x}$  compositions

Parameter	As content (at.%)						
	20	25	30	35	40	45	55
$E_s$ ( $\mu$ eV)	26.643	26.196	25.319	24.990	24.295	23.852	22.568
$A$	1,164.4	1,147.5	1,136.2	1,121.9	1,107.0	1,095.6	1,078.2

- iii. The conduction phenomena of the present alloys have emerged through two mechanisms. The thermally activated conduction through the extended states, which dominates in the relatively higher temperature range  $T > 233$  K and the hopping conduction through the localized states at relatively lower temperature range  $T \leq 233$  K.
- iv. The activation energy of electrical conductivity  $E_c$  was found to increase with increasing As content.
- v. The values of  $N(E_F)$ ,  $N$ ,  $R_{av}$  and  $W$  were found to be unsequentially and unreasonably high compared with those observed for some semiconducting materials and have been attributed to the incorrect assumptions of Mott's derivation of a VRH relations.

Finally the Seebeck coefficient possessed negative sign, which confirmed that the contribution to the observed TEP was mainly due to electrons. Moreover, the values of calculated  $E_s$  decreased with increasing As content which had been attributed to the decrease of electrons as the As content increases.

## References

- [1] G Luckovsky, F L Geleener, R H. Geils and R C Keezer *The structure of non-crystalline materials* P H Gaskell (London: Taylor and Francis) p 127 (1977)
- [2] M M Wakkad, E Kh Shokr and S H Mohamed *Phys. Status. Solidi (a)* **183** 399 (2001)
- [3] M M Wakkad, E Kh Shokr and S H Mohamed *J. Non-Cryst. Solids* **265** 157 (2000)
- [4] M M Wakkad *J. Therm. Anal. Calor.* **63** 533 (2001)
- [5] N K Rana and J N Prasad *Indian. J. Phys.* **86** 601(2012)
- [6] A M Ahmed, N M Megahid, M M Wakkad and A K Diab *J. Phys. Chem. Solids* **66** 1274 (2005)
- [7] R R Pawar, R A Bhavsar and S G Sonawane *Indian J. Phys.* **86** 871 (2012)
- [8] P S L Narasimham, A Giridhar and S Mahadevan *J. Non-Cryst. Solids* **43** 365 (1981)
- [9] Z U Borizova *Glassy Semiconductors* (New York: Plenum Press) (1981)
- [10] A Srinivasan and E S R Gopal *J. Mat. Sci.* **27** 4208 (1992)
- [11] O S Panwar, A Kumar, D R Goyal, K K Srivastava and K N Lakshminarayan *J. Non-Cryst. Solids* **30** 37 (1978)
- [12] E Marquez, P Villares and R Jimenez-Garay *J. Non-Cryst. Solids* **74** 195 (1985)
- [13] W Beyer and J Stuke *J. Non-Cryst. Solids* **8-10** 321 (1972)
- [14] S R Ovshinsky and H Fritzsche *Met. Trans.* **2** 641 (1971)
- [15] S Prakash, S Asokan and D B Ghare *J. Phys. D: Appl. Phys.* **29** 2004 (1996)
- [16] R M Mehra, A Pundir, A Kapoor and P C Mathur *J. Opt. (Paris)* **27** 139 (1996)
- [17] Z Yang, A A Wilhelm and P Lucas *J. Am. Ceram. Soc.* **93** 1941 (2010)
- [18] R A Narayanan, S Asokan and A Kumar *Phys. Rev. B* **54** 4413 (1996)
- [19] S H Mohamed, M M Wakkad, A M Ahmed and A K Diab *Eur. Phys. J. Appl. Phys.* **34** 165 (2006)
- [20] S R Elliot *Nature* **354** 445 (1991)
- [21] S R Elliot *physics of Amorphous Materials* 2nd ed. (Essex: Longman) p 71 (1990)
- [22] P E Lippens, J C Jumas, J Olivier-Fourcade, L Aldon, A Gheorghiu-de la Rocque and C. S  n  maud *J. Phys. Chim. Solids* **61** 1761 (2000)
- [23] J Vazquez, C Wagner, P Villares and R Jimenez-Garay *Mater. Chem. Phys.* **58** 187 (1999)
- [24] K Ramesh *J. Non-Cryst. Solids* **355** 2045 (2009)
- [25] A Abdel-aal, A Elshafie, M M El-Zaidia and A A Ammar *Physica B* **154** 105 (1988)
- [26] J Szeftel *Phil. Mag. B* **43** 549 (1981)
- [27] N F Mott and E A Davis *Electronic press in Non-Crystalline Materials* (Oxford: Clarendon press) (1979)
- [28] A Houg *Theoretical Solid State Physics* (Oxford: Pergaman Press) p 200 (1972)
- [29] P Nagels, E Sleenckx, R Callaerts and L Tichy *J. Solid State Commun.* **94** 49 (1993)
- [30] R M Mehra, R Shyam and P C Mathur *J. Non-Cryst. Solids* **31** 435 (1979)
- [31] A Giridhar, P S L Narasimham and S Mahadevan *J. Non-Cryst. Solids* **37** 165 (1980)
- [32] P S L Narasimham, A Giridhar and S Mahadevan *J. Non-Cryst. Solids* **43** 365 (1981); A Ghosh *Phys. Rev. B* **42** 5665 (1990)
- [33] D Lemoine and J Mendolia *Phys. Lett. A.* **82** 418 (1981)
- [34] M Cutler and N F Mott *Phys. Rev.* **181** 1336 (1969)
- [35] H Fritzsche *J. Non-Cryst. Solids* **6** 49 (1971)
- [36] Z Borizova *Glassy Semiconductors* (New York: Plenum) p 400 (1981)
- [37] A V Kolobov *J. Non-Cryst. Solids* **198-200** 728 (1996)
- [38] N Tohge, H Matsuo and T Minami *J. Non-Cryst. Solids* **95-96** 809 (1987)
- [39] B Vaidhyanathan, S Murugavel, S Asokan and K J Rao *J. Phys.Chem. B* **101** 9717 (1997)
- [40] N Asha Bhat and K S Sangunni *Solid State Commun.* **116** 297 (2000)
- [41] K Ramesh, M Prashantha, E S R Gopal and N Koteeswara Reddy *J. Appl. Phys.* **106** 113516 (2009)
- [42] J Tauc *Photo and thermoelectric effects in semiconductors* (New York: Pergamon) (1962)
- [43] A Ghosh *J. Appl. Phys.* **65** 227 (1989); N Tohge, T Minami and M Tanaka *J. Non-Cryst. Solids* **37** 23 (1980)
- [44] N F Mott, E A Davis and R A Street *Phil. Mag.* **32** 961 (1975)